Time Makes Space:
Emergence of Place Fields in Networks Encoding Temporally Continuous Sensory Experiences

Zhaoze Wang[1*]   **Ronald W. Di Tullio**[2*]   **Spencer Rooke**[3]   **Vijay Balasubramanian**[3,4,5]

[1]Department of Computer and Information Science, [2]Neuroscience, and [3]Physics,
University of Pennsylvania; [4]Rudolf Peierls Centre for Theoretical Physics, University of Oxford;
and [5]Santa Fe Institute   ∗: Equal contribution

zhaoze@seas.upenn.edu   ron.w.ditullio@gmail.com
srooke@sas.upenn.edu   vijay@physics.upenn.edu

Abstract

The vertebrate hippocampus is believed to use recurrent connectivity in area CA3 to support episodic memory recall from partial cues. This brain area also contains place cells, whose location-selective firing fields implement maps supporting spatial memory. Here we show that place cells emerge in networks trained to remember temporally continuous sensory episodes. We model CA3 as a recurrent autoencoder that recalls and reconstructs sensory experiences from noisy and partially occluded observations by agents traversing simulated arenas. The agents move in realistic trajectories modeled from rodents and environments are modeled as continuously varying, high-dimensional, sensory experience maps (spatially smoothed Gaussian random fields). Training our autoencoder to accurately pattern-complete and reconstruct sensory experiences with a constraint on total activity causes spatially localized firing fields, i.e., place cells, to emerge in the encoding layer. The emergent place fields reproduce key aspects of hippocampal phenomenology: a) remapping (maintenance of and reversion to distinct learned maps in different environments), implemented via repositioning of experience manifolds in the network's hidden layer, b) orthogonality of spatial representations in different arenas, c) robust place field emergence in differently shaped rooms, with single units showing multiple place fields in large or complex spaces, and d) slow representational drift of place fields. We argue that these results arise because continuous traversal of space makes sensory experience temporally continuous. We make testable predictions: a) rapidly changing sensory context will disrupt place fields, b) place fields will form even if recurrent connections are blocked, but reversion to previously learned representations upon remapping will be abolished, c) the dimension of temporally smooth experience sets the dimensionality of place fields, including during virtual navigation of abstract spaces. Code for our experiments is available at[1].

1   Introduction

The hippocampus is a brain region that plays a critical role in both spatial navigation [1, 2, 3] and episodic memory [4, 5, 6, 7, 8]. Researchers have therefore sought to understand the neural

---

[1]`https://zhaozewang.github.io/projects/time_makes_space`

substrates of these forms of memory in the hippocampus, as well as the extent to which these roles are interrelated [9, 10, 11, 12]. A key role is played by place cells – so named because they fire in specific spatial locations within an environment [13]. Place cells have spatially constrained firing fields, and "remap" firing patterns in response to significant contextual changes (especially in hippocampal subregion CA3) [14, 15, 16, 17, 18, 19], including motion to a new environment [20] and modified behavioral context or sensory cues [21, 22]. After remapping, they form almost orthogonal representations [21, 23]. These findings suggest that CA3 place cell network may play a key role in maintaining both positional and contextual information [19, 24], while also supporting a large capacity for memory storage [25]. Meanwhile, others have suggested that hippocampal CA3 is a pattern completion and separation device [26, 27, 28, 29] that supports the storage and retrieval of episodic memories from partial cues [30, 7, 29]. This claim is supported by the extensive recurrent collaterals in CA3 [31, 32, 7], which could allow it to act as an autoassociative network retrieving a complete memory fron partial cues [33, 34, 7, 29].

Prior studies reconciling the spatial and episodic memory perspectives on CA3 propose that hippocampus associates sensory cues with spatial information [35, 36, 37, 38]. In this view, given partial sensory signals, CA3 recalls and reconstructs associated spatial information. Benna and Fusi [39] proposed the hippocampus as a memory compression device, contrasting and memorizing differences between multiple visits to a room, and showed that autoencoders with sparsity constraints develop place-like representations in the network encoding layer. Likewise [40] suggests that spatial awareness results from processing sequences of sensory inputs, and in a learning framework based on Hidden Markov Models, observed the emergence of place-like patterns. Furthermore, [41] trained an RNN on visual observations conditioned on the agent's direction to predict near-future observations and also found localized spatial representations. However, several questions remain. What signals contribute to spatial information? How are memories from multiple visits compared? Do such frameworks reproduce the phenomenology of place cells, including remapping and reversion across rooms during realistic navigation to create orthogonal representations?

Here, we propose that sensory cues weakly modulated by spatial locations collectively create spatial information, and that auto-associating these signals during spatial traversal elicits emergence of place-like patterns. We test this idea by simulating an artificial agent that receives partial and noisy sensory observations while traversing simulated rooms. We model CA3 as a recurrent autoencoder (RAE), which tries to reconstruct complete sensory experiences given partial and noisy observations at each location. We find that place-like firing patterns closely resembling rodent hippocampal place cells emerge in the encoding layer of this RAE. This emergence does not require explicit sparsity constraints (unlike [39]) and is robust across a wide range of environmental geometries, numbers of encoding units, and dimensions of sensory cues. We demonstrate that the pattern-completion objective encourages encoding units to prioritize temporally stable components of perceived experiences, naturally forming place-like representations. We also find that learned recurrent connections reflect expected variations of sensory experience, and thus enable single cells to form distinct representations of sensory experiences at similar locations in different environments. This mechanism allows our emergent place cells to remap and revert spatial representations when agents move between multiple unfamiliar and familiar environments, resembling place cells in the brain [42, 43, 22]. Finally, similar to place cells in CA3, our emergent place units form uncorrelated representations for different rooms and maintain these representations over an extended period.

Our model predicts that: (1) Rapidly varying sensory experience across space will disrupt place field formation; (2) Disrupting CA3 recurrent connections will not disrupt place fields, but will reduce the speed of formation of new spatial representations and prevent reversion to previous configurations upon re-entry of familiar rooms; (3) The temporally smooth components of sensory experience sets the dimensionality of place fields for animals traversing physical or abstract spaces.

2 Method

2.1 Episodic memory during spatial traversal

We first construct a framework for modeling episodic memory, then predict behavior during navigation. First, assume that the hippocampus continuously receives inputs from other cortical areas such as the entorhinal cortex, prefrontal cortex, and thalamus [44, 45, 7, 1], collectively constituting a high-dimensional experience vector (EV), a point in an abstract space of possible experiences $\mathbb{E}$. An
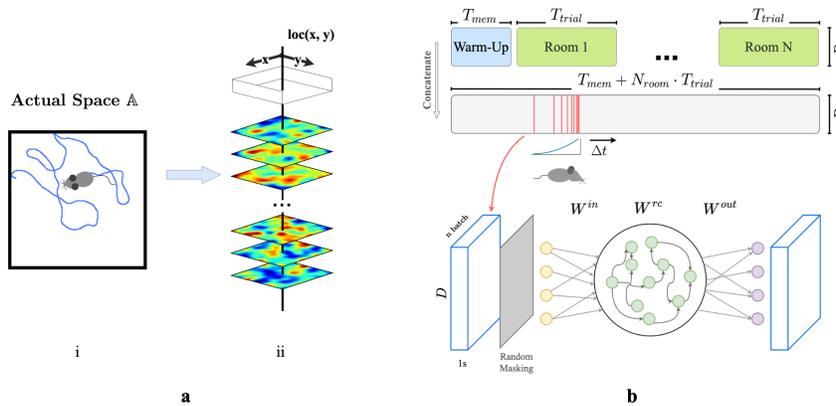
Figure 1: **a.** (i) Example trajectory of an artificial agent in a 2D room in actual space $\mathbb{A}$. (ii) Each room is defined by a unique set of weakly spatial modulated (WSM) signals representing location-dependent sensory cues. Within a room, a WSM rate map is defined by $F = z * g(\sigma), F \in \mathbb{R}^{W \times H}$, where z is a 2D Gaussian random field. W and H are the dimensions of the room. A room is defined by its WSM set, i.e., $R = [F_1, F_2, \cdots, F_D]^\top, R \in \mathbb{R}^{D \times W \times H}$. **b.** Training schematic of our RAE. An artificial agent explores room(s) defined by a unique set of WSM signals, as depicted in panel **a**. Agents receive location-specific sensory experience vectors $\mathbf{e}_{x,y} = R[:, x, y]$, where $\mathbf{e}_{x,y} \in \mathbb{R}^D$. The agent's trajectory within a trial is thereby converted into a sequence of experience vectors. At every training step, we randomly sample N_{batch} segments of T_s seconds from episodic memories within a T_w second window. These segments form a stack of memories used to train the RAE. Every EV in this stack is randomly masked to occlude between r_{min} to $r_{max}\%$ of the signal with added Gaussian noise ϵ. The RAE is trained to reconstruct complete, noiseless experience vectors. The sampling window is shifted forward by Δt after each step until the end of the trial.

agent experiences this world through a temporal sequence of "events". Each event produces a short sequence of EVs - a 'segment' of episodic memory. A single event of bounded duration should trace a brief, continuous trajectory in the experience space $\mathbb{E}$. Formally, let $\mathbf{E} = \{\mathbf{e}_0, \mathbf{e}_1, \ldots, \mathbf{e}_T\}$ represent the segment of episodic memory generated by a single event, where each $\mathbf{e}_t \in \mathbb{R}^D$ (for $t = 0, 1, \ldots, T$) denotes an EV at time t, D is the dimension of the input experience space, and T is the duration of this episode in discrete time steps. We take each time step to represent 50 ms in real-time. The sequence is continuous such that for any t and $t + 1$, where $0 \leq t < T$, there exists a non-zero correlation coefficient, $\rho(\mathbf{e}_t, \mathbf{e}_{t+1})$. During spatial navigation, we expect the environment to be temporally stable, with location-dependent experiences. We therefore model EVs in a fixed room as weakly spatial modulated (WSM) signals (Fig. 1), defining a manifold in the experience space $\mathbb{E}$. In this view, episodic memories of traversal of an environment sample the WSM manifold that defines it.

2.2 Recurrent Autoencoder (RAE) as a model of pattern completion and separation

We then construct a simple network model of CA3 for recalling and pattern-completing arbitrary experience vectors. We train the network on EVs generated by an artificial agent exploring varied environments. We design the network following classical theories of CA3 for episodic memory storage, which suggest that recurrent collaterals of CA3 [46, 31, 32, 17, 29] develop attractor dynamics [47] enabling association of similar patterns and separation of dissimilar ones [37, 28, 29]. Accordingly, we model CA3 as a recurrent autoencoder (RAE). In view of previous research that observed emergence of grid-like patterns in recurrent neural networks (RNNs) trained for navigation [48, 49, 50], we implemented our RAE as a continuous-time RNN. Input projections denoted as W^{in} represent pathways entering the hippocampus (Fig. 1b). The hidden layer units use a ReLU non-linearity and contain recurrent connections W^{rc}, emulating non-linear responses in CA3 neurons and their recurrent collaterals. The network then uses post-synaptic connections W^{out} representing CA3's projection to other brain regions to decode hidden unit states. All weight matrices W^{in}, W^{rc}, and W^{out} are initialized to a zero mean uniform distribution (Suppl. Sec. 1). In this formulation, both direct and disynaptic inhibition, the latter via interneurons, are represented as negative weights.

During each trial, agents sampled from the unique set of WSM signals that defined that environment. (Fig. 1a.i & ii), while moving in trajectories that imitated rodents (random walks with low-probability changes of direction and speed, see Suppl. Sec. 1). We discretized each T_t trial into dt timesteps during which agents received location-specific local EVs with elements randomly masked to imitate factors limiting observation like occlusion and partial attention. We concatenated timesteps sampled from a decaying distribution (Suppl. Sec. 1.2) of recent experiences (Fig. 1b) into 'episodic bouts' and trained the RAE on these bouts. We added pre- and post-activation noise to the hidden layer to simulate variability inherent to sensory processing. The use of episodic bouts serves to encourage input/output projections to update in consideration of events from a more extended history. We use a mean-squared error (MSE) objective function for pattern completion and an MSE constraint on the total hidden layer firing rates to enforce realistic firing rates.

After a trial ends, we "record" from the network by letting the agent run freely in the trial room while gathering firing patterns of units within the network (Suppl. Sec. 1). During this recording block, we pause RAE updates so no additional learning occurs. We analyze the recorded firing patterns in the same way as experimentally recorded place cells, by projecting onto 2D room maps for visualization (Suppl. Sec. 1.3) and calculating the Spatial Information Content (SIC, see Suppl. Sec 2.1) [51].

3 Results

3.1 Emergence of place-like patterns

Fig. 2 displays firing profiles of 40 random hidden units, with their spatial information content indicated above. A significant number of cells display strong place-like firing patterns. For example, consider a typical choice of training and constraint parameters (Suppl. Sec. 1.2), for which ∼10% of the hidden units are active with average firing rates above a threshold of 0.1 Hz. We find in these cases that ∼80% of the active hidden units have SIC greater than 5, which is 20 times the SIC of the WSM inputs (0.29 ± 0.01; mean $\pm$ SD). Thus, place-like cells emerge from dynamics of the task and network structure. The parameters we used in our experiments are in Suppl. Sec. 1.2, while we also verified that their precise values do not impact the emergence of place fields (Suppl. Sec. 4.2).
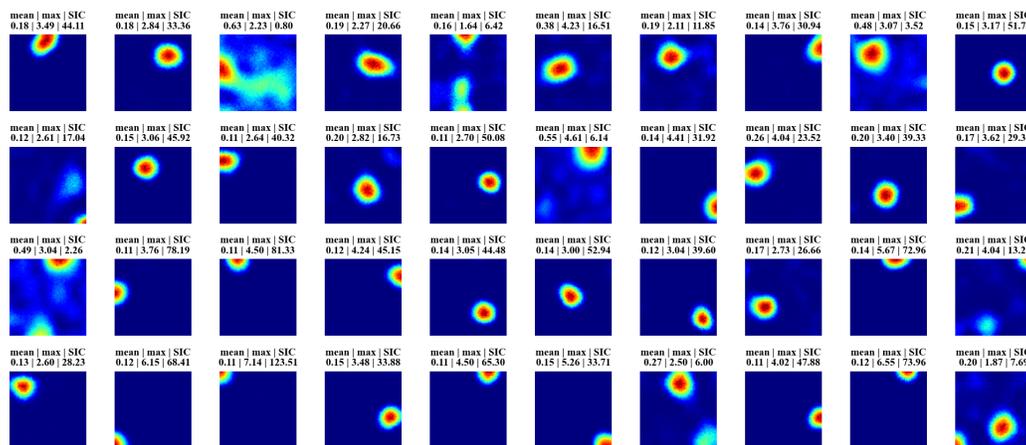

Figure 2: Firing maps of 40 randomly selected units in a trial room. A majority demonstrate clear place-like firing patterns. Subplot labels indicate the mean and max firing statistics of each unit in Hz. The spatial information content is indicated in the last column of subplot labels.

3.2 Place field emergence reflects temporally continuous changes in sensory experiences

We describe environments through weakly spatially modulated (WSM) sensory experience profiles that translate physical locations to points in experience space, $\mathbb{E}$. WSM signals are spatio-temporally continuous, so smooth motions between adjacent locations generate smooth motions in $\mathbb{E}$. Thus an agent's exploration generates a set of trajectories in $\mathbb{E}$ that are unique to each environment and the agent's paths. The set of possible trajectories the agent could take together defines a surface in $\mathbb{E}$,

the experience manifold (EM) of an environment. This manifold has the dimension of the space of accessible sensory experiences. Thus, an agent in a 2D room generates a 2D experience manifold.

First consider neurons without recurrent connections. Given n-dimensional inputs, each neuron's input projection and ReLU non-linear firing rate collectively define an activation boundary (AB), an $n-1$ dimensional plane dividing the experience space $\mathbb{E}$. This boundary occurs at input loci where the neuron transitions from inactive to active. More generally, the distance of an input $\mathbf{e}$ to a neuron's activation boundary determines the response firing rate, regardless of the activation function. For example, in Fig. 3b & c, an animal traversing a 1D track traces an EM within a 2D experience space. The EM is encoded by two neurons, $N1$ (Fig. 3c.i) and $N2$ (Fig. 3c.iii), with the indicated ABs. As an animal moves from $loc1$ to $loc2$, its perceived experience moves along EM and intersects $N1$'s activation boundary. This motion causes $N1$'s firing rate to gradually increase then decrease (Fig. 3c.ii). In contrast, $N2$'s activation boundary is roughly perpendicular to the same EM, motion from $loc1$ and $loc2$ will change neuron $N2$'s firing rate monotonically (Fig. 3c.iv).

Our autoencoder linearly decodes sensory experience from the hidden unit activations as $\hat{\mathbf{e}} = \sum_{j \in S} r_j \mathbf{W}_j^{out}$ where j indexes hidden units, $\mathbf{W}_j^{out}$ is the output weight vector and S are units that fire at the given location. If the firing rate of a unit i increases monotonically as an agent moves along the EM, the angle between $\hat{\mathbf{e}}$ and the experience encoded by unit i, $\mathbf{W}_i^{out}$, will decrease monotonically as this unit dominates. This will cause the reconstructed experience at many locations to be dominated by a single vector which cannot generally be correct. On the other hand, if the activation boundary for a unit is exactly parallel to an EM, it will have the same firing rate everywhere and will not contribute to discriminating locations. Thus, the most useful units for reconstructing sensory experience will have activation boundaries segmenting the EM like $N1$ in Fig. 3c.i.
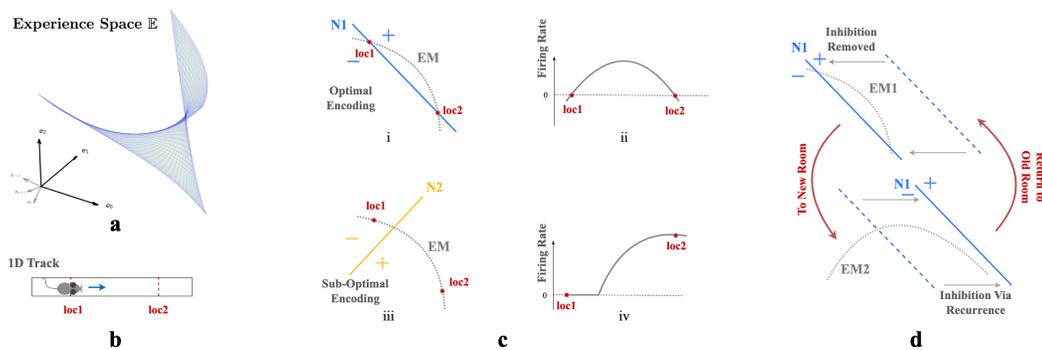

Figure 3: **a.** A room is defined by a unique set of WSM signals describing expected sensory experience at every location. The set of WSM signals converts a room to a hyperplane in experience space. **b.** Illustration of animal moving from $loc1$ to $loc2$ in a 1D track. **c.** i & iii) Illustration of two neurons $N1$ and $N2$ intersecting the experience manifold EM corresponds to the 1D track. ii & iv) Corresponding firing rates as the animal moves from $loc1$ to $loc2$. **d.** EM1 and EM2 are two experience manifolds corresponding to two rooms. The optimal encoding neuron for EM1 may be temporarily inhibited through recurrent connections when entering a new room, then reactivated upon returning to the previous room.

This argument implies that training should rotate activation boundaries of some hidden units to segment the generally nonlinear experience manifold (EM). To simultaneously encode similar but differently positioned EMs (Fig 3d), in networks without recurrent connections, neurons would require substantial rewiring of input projections W^{in}. Recurrence helps reallocate the contributions to reconstructed sensory experience, so that the largest contributions are made by units whose activation boundaries segment the EM. This switching of encoding neurons obviates the need for input projection rewiring.

We can also see from this reasoning why place-like units develop in the hidden layers. A given hidden unit contributes $\hat{\mathbf{e}}_i = r_i W_i^{out}$ to the reconstructed experience. As we explained above, only hidden units whose activation boundaries segment the EM are useful for reconstructing experience, so learning will either rotate activation boundaries to segment the EM, or adapt output weights W_i^{out} to remove the unit from the reconstruction. Consider the location of peak firing of a unit whose

planar activation boundary intersects the curved EM as in Fig. 3c.i. Because of the continuity of the EM, adjacent locations will produce similar experiences. The region of space where the unit fires will correspond to the part of the EM that is segmented by the activation boundary (indicated by '+' in Fig. 3c & d). Assuming that the component of the experience vector that is orthogonal to the activation boundary varies approximately isotropically in space, the intersection locus of the activation boundary with the EM will be approximately circular when projected back to the environment. Thus, a population of such units, each tuned to part of the temporally continuous variation of experience, will exhibit place-field-like activation regions.

Critically, as we argued, the presence of recurrent inhibitory connections enables units that are most useful in one room to remain silent in other rooms. Recurrent inhibitory connections allow neurons to do this **without altering their activation boundaries, i.e., input projections**. So when an animal reenters a familiar room, both the room's EM and input projections to each neuron will remain relatively stable, while the recurrent connections reactive the most useful neurons in this familiar room. This combination ensures that individual neurons have stable place fields within a particular room while maintaining flexibility in the network to encode multiple rooms. This stability occurs because the relative positions of the EM of a familiar room and the activation boundaries of the encoding neurons remain unchanged. Thus radical changes to experiences within a familiar room could still induce change, as is observed experimentally [16, 24].

3.3 Place cell remapping as EM repositioning

We then tested whether our networks support place cell remapping across rooms and reversion within familiar rooms. To do so, we extended our experiment in Sec. 3.1 by simulating agents exploring two rooms over three sessions in a sequence R1-R2-R1, where R1 and R2 are rooms defined by unique WSM signals. After training in each room, we recorded hidden layer firing patterns. The results were labeled T1R1, T2R2, and T3R1, representing the Trial (T) and Room (R), respectively.

We selected active hidden units (mean firing threshold ≥ 0.1 Hz) across trials with SIC above 5 (more than 20x the SIC of the WSM signal) for comparison. T2R2 demonstrates significant remapping in hidden nodes as compared to T1R1 (upper row of Figs. 4a, 4b). Hidden nodes displayed both global and partial remapping with many nodes displaying global remapping including: in the given example, ceasing to fire (n=39), beginning to fire (n=94), or consistently firing in both rooms (n=130). We also observed place firing fields reverting to their original locations, upon returning to room 1 (T3R1) (Figs. 4a,4b, lower rows). These results mirror observations in rodent hippocampus CA3 [18, 20, 21]. To quantify, we calculated pairwise Pearson correlations of firing fields for the selected hidden layer units (Fig. 4b). The correlation matrix showed low spatial correlation in firing fields between T1R1 and T2R2. By contrast, the correlation matrix of T1R1 and T3R1 showed significantly higher diagonal values, indicating reversion of place fields in a familiar enclosure.

We then tested the mechanism of reversion. To do so, we calculated a reorganization score s of the input projections (W^{in}) and recurrent connections (W^{rc}) across trials (see Suppl. Sec. 2.2). Transitioning from T1R1 to T2R2, we observed a substantial reorganization of W^{rc} ($s = 0.564$) but only minor alterations in input projections W^{in} ($s = 0.169$). Between T2R2 and T3R1, W^{in} also exhibits small changes ($s= 0.141$), whereas W^{rc} continues to show a higher reorganization of $s = 0.430$. This observation is consistent with experimental results indicating that synapses between hippocampal neurons in the same region update at a much faster rate than synapses coming from neurons projecting to the hippocampus or across hippocampal regions [52], and confirms that in our model remapping and reversion are driven by reorganization of recurrent connections.

In our framework, different rooms might correspond to differently positioned experience manifolds (EMs) in $\mathbb{E}$. We suppose the network has sufficient capacity to encode every EV in experience space $\mathbb{E}$, and thus every volumetric region in $\mathbb{E}$ (small cubes in Fig. 4c) is encoded by some neurons, similar to what we described in Fig. 3b. Then, moving between rooms R1 and R2 (blue and orange planes in Fig. 4c) induces two potential remapping scenarios: (a) Neurons encoding a volumetric region intersect with only one room's manifold – activating in R1 and remaining inactive in R2 (magenta region), and vice versa for R2 (cyan region), (b) Both manifolds intersect a given region (red cube in Fig. 4c), and will activate in different physical locations for each room (shifting firing centers). Alternatively, intersections at similar locations from different angles or positional shifts can cause neurons to adjust their firing rates or alter their patterns (rate changes or partial remapping).
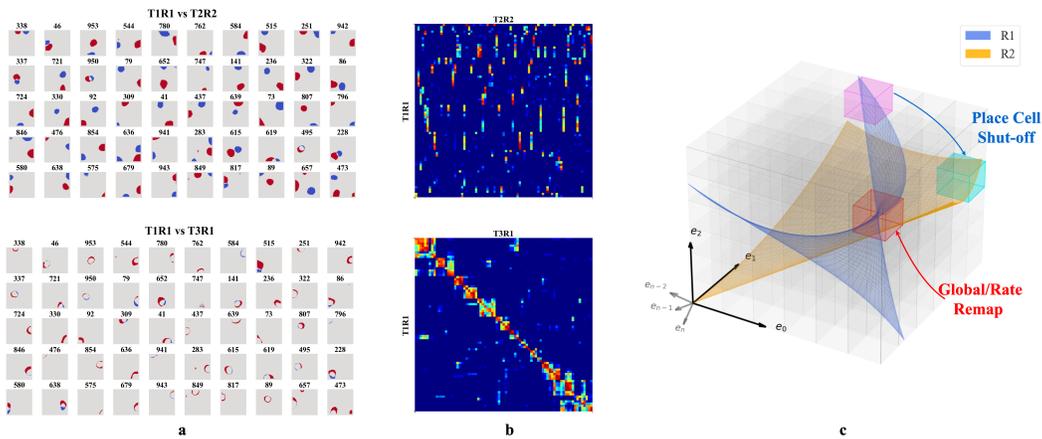
Figure 4: **a-b.** Firing profiles of hidden units that fire (mean firing threshold=0.10 Hz) in all three trials and have a place score greater than 5. *Upper row:* Comparison of T1R1 and T2R2. *Lower row:* T1R1 vs. T3R1. **a.** We select cells that fire in all three trials and construct maps of the difference in the binarized firing fields for different rooms (R1 - R2) to compare their locations of firing. The firing fields are binarized by thresholding at 20% of the maximum firing rate of each unit. **b.** Pearson correlations of the firing fields sorted using hierarchical clustering for visual clarity. **c.** Illustration of experience manifolds from two rooms. Moving from room R1 to R2: the encoding units for the magenta region cease firing while those for the cyan one start firing. The encoding units for the red volume fire in both rooms. However, the EMs of R1 and R2 might intersect at different angles or correspond to different spatial locations, thereby undergoing global/rate remapping.

3.4 Storage capacity and the orthogonality of spatial representations

Studies of episodic and spatial memory suggest that CA3 can memorize and discriminate a large number of experiences [18, 21]. Thus, we tested whether our network can also encode a large number of rooms in orthogonal representations. To do so, we expanded our training protocol to include 20 unique rooms. We call a complete visit of all 20 rooms a "cycle" and trained the RAE for 30 cycles, with the room sequence shuffled in each cycle. We reduced the time the agent spent in each room to 10 minutes (12000 timesteps) to avoid overfitting to a single room while training. This trial duration still exceeds the experience sampling window size of 5 minutes (see Fig. 1 caption), ensuring a period in which the RAE receives experiences exclusively from one room.

After each trial, we replicated analyses in [21] to compare hidden layer population coding vectors in different rooms. For each room, we employed a 5×5 cm binning window to discretize each 100×100 cm firing rate map across all 1000 hidden units, resulting in a population vector with dimensions $N \times W \times H = 1000 \times 20 \times 20$. We compared the similarity between any two population vectors by their Pearson correlation coefficients (Suppl. Sec. 3.1).

We compared the correlation between rooms from cycle 2 and cycle 3, a scenario similar to the experiments in [21]. The mean correlation between different rooms is 0.164 ± 0.029, and that of the same rooms is about 0.55 greater, 0.710 ± 0.097. The corresponding experimental values reported in [21] are also different by about 0.57: 0.08 ± 0.005 and 0.65 ± 0.02, respectively. Note that we should not expect precisely the same values of the correlation because the precise setups of the environments and experiments are different. For example, we have many trial rooms in our *in silico* study, while there are only 2 rooms in [21]. Furthermore, our network contains 1000 units while Alme et al. recorded only 342 neurons [21]. Overall, we find that the population vectors of familiar rooms have significantly higher correlations as compared to different rooms, consistently with experiments [21, 18, 16, 19, 23]. We also observed that the correlation between population vectors from consecutive visits to the same room quickly stabilizes, exceeding 0.8 after the third cycle (Fig. 5a). These results combine to suggest that our network is capable of stably encoding a large number of rooms in orthogonal representations.

We also observed gradual drifts in the generated place fields as well as a slow decrease across cycles in correlation with the initial representations, in parallel with recent experiments suggesting that
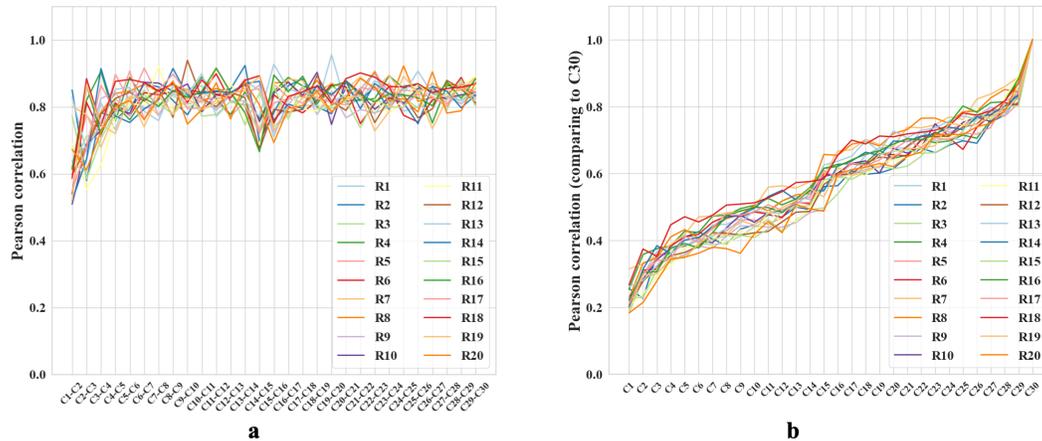
Figure 5: **a-b.** Colored lines = data from different trial rooms. **a.** Change in Pearson correlation of population vectors for the same room across consecutive cycles. C_n-C_{n+1} compares two subsequent cycles. **b.** Pearson correlation of population vectors from various cycles compared with the final cycle for different rooms. Cycle 1 is excluded because the place fields are not fully formed. As the cycle number increases, the correlation coefficients also increase.

place cells in the brain have representational drift reflecting continuous learning processes [53]. We propose that drifts in our network also reflect incremental learning of more efficient ways to encode multiple rooms. To explore, we measured the amount of reversion (Pearson correlation with previous firing patterns) during the first few moments of reintroduction to a familiar room. During early cycles, such as the third cycle, reintroduction to a familiar room results in a delayed reversion of the place fields (Pearson correlation $r = 0.35$ when the agent enters a familiar room). During the final cycle, cycle 30, the fields immediately reverted to their original patterns upon reentry ($r = 0.92$), supporting our proposal. Additional comparisons, including plots of place field drifts, appear in Suppl. Sec. 3.2.

3.5 Robust emergence of place fields and multiple place fields in larger rooms.

While we primarily tested our network in $1\text{m} \times 1\text{m}$ square rooms, we have confirmed that place fields robustly emerge in environments of various shapes (Suppl. Sec. 4). We also found that emergence of place fields is robust to the dimension of the experience vectors and the number of hidden units (Suppl. Sec. 4). There is experimental evidence that place cells can develop multiple place field centers in larger enclosures [54, 55]. We tested whether this phenomenon occurred within our RAE. To do so, we had our agent explore an environment that contained two rooms connected by a tunnel and trained our RAE on the resulting experiences (Fig. 6a). Mirroring experimental results, some units in the hidden layer of our RAE developed more than one firing center.

4 Predictions

Our theory generates several testable predictions. First, we predict that rapid changes to sensory and contextual experiences within an environment will disrupt and destabilize place fields. This prediction emerges from the results of Sec. 3.2, where we showed that neurons would orient their firing patterns to encode the most varying direction of experience vectors (EVs) at adjacent physical locations. If EVs at neighboring locations exhibit substantial variations over short durations of time, there is no consistent, most varying direction of the EVs. Accordingly, it is impossible for place cells to effectively learn temporal variance at adjacent locations, leading to an interruption in the formation of place cells. This prediction can be readily tested in VR setups as well as in specially constructed physical environments. Spatial information or other metrics of place cell stability should be measured as a function of sensory/contextual experience change. We anticipate a negative correlation that place cell stability decreases as more aspects of the experience are changed. Secondly, expanding on our hypothesis from Sec. 3.1, which suggests that recurrent connections facilitate reversion of place fields, we propose that the absence of recurrent connections will not disrupt formation of place fields, but will prevent them from reverting to previous representations upon re-entry into
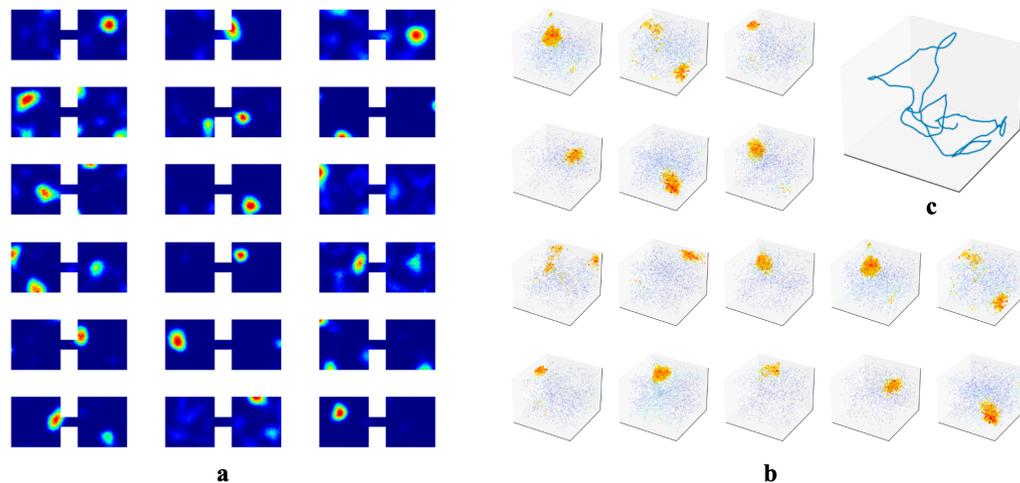
Figure 6: **a.** Example hidden unit firing maps from a model trained in two connected 1m × 1m square rooms. The rooms are connected by a 20cm × 10cm tunnel. **b-c** To test whether the agent could generate 3D place fields, we assume the agent is able to travel freely in 3D spaces similar to its movement in 2D rooms. We increased the number of WSM channels to 1000 to increase experience specificity in 3D enclosures. **b.** Placing artificial agents in 3D rooms defined by 3D WSM signals, we observed an emergence of 3D place fields. Locations where neurons fire above 65% max firing rate are densely plotted. 1% of the remaining locations are randomly selected and plotted to indicate neurons firing at these locations. Warmer colors indicate higher firing rates.

a familiar room, a prediction testable by silencing of recurrent hippocampal connections. Third, it is known that deforming a room by stretching or shrinking it changes the firing fields of grid cells [56, 57, 58, 59] and correspondingly affects human behavior [60], possibly because grid fields depend on path integration [61, 62], and there are trajectory dependent shifts in their locations driven by interaction with border cells [63, 64]. Grid cells provide one important class of inputs to the hippocampus, and so we expect that the changed grid cell input will correspondingly deform the experience manifold. Our model predicts the corresponding statistics of partial remapping of place fields when the familiar but deformed room is revisited.

We also predict that the dimensionality of place fields is determined by the dimension in which temporally stable experiences change smoothly. As outlined in Sec. 3.2, place cells in our network prioritize encoding the most variable component within a localized region. The dimensionality of emergent place cells is therefore set by the projection of this encoded component onto the experience manifold (EM), and will be defined by the number of independent components of experience that change smoothly as an animal moves through a space—whether physical or abstract. To substantiate, we simulated an agent in 3D rooms and trained our RAE, similar to Sec. 3.1. We observed the emergence of 3D place fields (Fig. 6b). This prediction is indirectly confirmed by Grieves et al. [65], who observed 3D place cells in rodents navigating a lattice maze, a 3D environment that where rodents explore volumetrically. To test in physical spaces, VR setups with parametrically controlled sensory inputs could be employed. For abstract space, the prediction could be tested following procedures similar to the bird-deformation space used in Constantinescu et al. [66], or by placing rodents in 1D or 2D tracks while gradually changing auditory/olfactory signals within the enclosure or varying visual cues displayed on walls. We predict these continuous changes along the abstract dimension will extend previously generated place cells to higher dimensions.

5   Discussion

In our study, we tested how episodic and spatial memory, as implemented in the hippocampus, could be interrelated and complementary. To do so, we constructed a recurrent autoencoder (RAE) model of CA3 that received partial and noisy sensory inputs while an agent traversing an environment attempted to reconstruct the complete sensory experience at each location based on previous encounters. We

demonstrated that networks concurrently minimizing average firing rate and reconstruction error naturally develop place-like responses. These responses create a continuous landscape of attractor basins (Suppl. Sec. 4.3), enabling robust recall of spatial experience at any location. We found that the emergent place-like units display remapping resembling experiments [21, 17, 18, 29], including cells that only fire in some environments while turning off in others, and other that change their firing location in novel environments while reverting in familiar arenas. Our network also generates orthogonal spatial representations for multiple rooms similarly to place cells in the brain.

Our findings both reinforce and reframe previous theories of place cell generation, place cell remapping, and CA3 function. Previous works have discussed how sensory or contextual information could be multiplexed with purely spatial information [29, 23]. While both types of information can be encoded in the CA3 place cell network, our theory suggests a unified "sensory as spatial" framework, which leverages the fact that particular combinations of sensory experiences tend to happen at particular locations and that sensory experiences tend to change smoothly over time. Neurally, these facts are embodied in the numerous weakly spatially modulated cells seen as inputs to the hippocampus [67] and which we use as the input to our network. We accordingly propose that these inputs are the primary drivers of place cell generation.

In our model, neurons that capture more input variance contribute more to pattern completion, and reorganization of recurrent connections serves to maximize their role. This suggests that individual cells will remap to form unique representations for similar sensory experiences encountered in different environments since the trajectory of those experiences and the expected variation of these experiences will differ across rooms. At a network level, this difference is reflected in reorganization of recurrent connections across environments, along with minimal input projection adaptation. These input projections also allow experience trajectories to remain stable in familiar environments, allowing cells to revert to prior firing locations upon return to a familiar arena. Finally, our findings indicate that if a network repeatedly navigates between multiple rooms, it could gradually learn to encode them more efficiently, enabling immediate remapping without learning/rewiring recurrent connections.

Our study provides a simple yet powerful framework that reproduces a substantial part of the phenomenology of place cells. It would be interesting to statistically compare our emergent place cells with rodent hippocampus data especially if we can also accumulate "natural experience statistics" from multi-modal sensors attached to navigating physical agents.

References

[1] James J. Knierim. The hippocampus. *Current Biology*, 25(23):R1116–R1121, December 2015.

[2] May-Britt Moser, David C. Rowland, and Edvard I. Moser. Place Cells, Grid Cells, and Memory. *Cold Spring Harbor Perspectives in Biology*, 7(2):a021808, February 2015.

[3] Edvard I Moser, May-Britt Moser, and Bruce L. McNaughton. Spatial representation in the hippocampal formation: A history. *Nature Neuroscience*, 20(11):1448–1464, November 2017.

[4] Larry R. Squire and Carolyn Backer Cave. The hippocampus, memory, and space. *Hippocampus*, 1(3):269–271, July 1991.

[5] Suzanne Corkin. What's new with the amnesic patient H.M.? *Nature Reviews Neuroscience*, 3(2):153–160, February 2002.

[6] Larry R. Squire. The Legacy of Patient H.M. for Neuroscience. *Neuron*, 61(1):6–9, January 2009.

[7] Michael E. Hasselmo. *How We Remember: Brain Mechanisms of Episodic Memory*. The MIT Press, 2011.

[8] Michael E. Hasselmo and Chantal E. Stern. Theta rhythm and the encoding and retrieval of space and time. *NeuroImage*, 85:656–666, January 2014.

[9] Howard Eichenbaum and Neal J. Cohen. Can We Reconcile the Declarative Memory and Spatial Navigation Views on Hippocampal Function? *Neuron*, 83(4):764–770, August 2014.

[10] Michael E. Hasselmo, James R. Hinman, Holger Dannenberg, and Chantal E. Stern. Models of spatial and temporal dimensions of memory. *Current Opinion in Behavioral Sciences*, 17:27–33, October 2017.

[11] Howard Eichenbaum. On the Integration of Space, Time, and Memory. *Neuron*, 95(5):1007–1018, August 2017.

[12] James Cr Whittington, Timothy H Muller, Shirley Mark, Guifen Chen, Caswell Barry, Neil Burgess, and Timothy Ej Behrens. The Tolman-Eichenbaum Machine: Unifying space and relational memory through generalisation in the hippocampal formation, September 2019.

[13] J. O'Keefe and J. Dostrovsky. The hippocampus as a spatial map. Preliminary evidence from unit activity in the freely-moving rat. *Brain Research*, 34(1):171–175, November 1971.

[14] Robert U. and John L. Kubie. The effects of changes in the environment on the spatial firing of hippocampal complex-spike cells. *The Journal of Neuroscience*, 7(7):1951–1968, July 1987.

[15] Elizabeth Bostock, Robert U. Muller, and John L. Kubie. Experience-dependent modifications of hippocampal place cell firing. *Hippocampus*, 1(2):193–205, April 1991.

[16] Karel Jezek, Espen J. Henriksen, Alessandro Treves, Edvard I. Moser, and May-Britt Moser. Theta-paced flickering between place-cell maps in the hippocampus. *Nature*, 478(7368):246–249, October 2011.

[17] Trygve Solstad, Hosam N. Yousif, and Terrence J. Sejnowski. Place Cell Rate Remapping by CA3 Recurrent Collaterals. *PLoS Computational Biology*, 10(6):e1003648, June 2014.

[18] Stefan Leutgeb and Jill K. Leutgeb. Remapping to discriminate contexts with hippocampal population codes. In *Space,Time and Memory in the Hippocampal Formation*, pages 227–251. Springer Vienna, Vienna, 2014.

[19] Shirley Mark, Sandro Romani, Karel Jezek, and Misha Tsodyks. Theta-paced flickering between place-cell maps in the hippocampus: A model based on short-term synaptic plasticity. *Hippocampus*, 27(9):959–970, September 2017.

[20] John O'Keefe and Lynn Nadel. *The Hippocampus as a Cognitive Map*. Clarendon Press ; Oxford University Press, Oxford : New York, 1978.

[21] Charlotte B. Alme, Chenglin Miao, Karel Jezek, Alessandro Treves, Edvard I. Moser, and May-Britt Moser. Place cells in the hippocampus: Eleven maps for eleven rooms. *Proceedings of the National Academy of Sciences*, 111(52):18428–18435, December 2014.

[22] John L. Kubie, Eliott R. J. Levy, and André A. Fenton. Is hippocampal remapping the physiological basis for context? *Hippocampus*, 30(8):851–864, August 2020.

[23] Lorenzo Posani, Simona Cocco, Karel Ježek, and Rémi Monasson. Functional connectivity models for decoding of spatial representations from hippocampal CA1 recordings. *Journal of Computational Neuroscience*, 43(1):17–33, August 2017.

[24] Lorenzo Posani, Simona Cocco, and Rémi Monasson. Integration and multiplexing of positional and contextual information by the hippocampal network. *PLOS Computational Biology*, 14(8):e1006320, August 2018.

[25] Aldo Battista and Rémi Monasson. Capacity-resolution trade-off in the optimal learning of multiple low-dimensional manifolds by attractor neural networks. *Phys. Rev. Lett.*, 124:048302, Jan 2020.

[26] David Marr. Simple memory: A theory for archicortex. *Philosophical Transactions of the Royal Society of London. B, Biological Sciences*, 262(841):23–81, July 1971.

[27] Michael A. Yassa and Craig E.L. Stark. Pattern separation in the hippocampus. *Trends in Neurosciences*, 34(10):515–525, October 2011.

[28] Edmund T. Rolls. The mechanisms for pattern completion and pattern separation in the hippocampus. *Frontiers in Systems Neuroscience*, 7, 2013.

[29] James J. Knierim and Joshua P. Neunuebel. Tracking the flow of hippocampal computation: Pattern separation, pattern completion, and attractor dynamics. *Neurobiology of Learning and Memory*, 129:38–49, March 2016.

[30] Edmund T. Rolls. A computational theory of episodic memory formation in the hippocampus. *Behavioural Brain Research*, 215(2):180–196, December 2010.

[31] X.-G. Li, P. Somogyi, A. Ylinen, and G. Buzsáki. The hippocampal CA3 network: An in vivo intracellular labeling study. *Journal of Comparative Neurology*, 339(2):181–208, January 1994.

[32] Menno P. Witter. Intrinsic and extrinsic wiring of CA3: Indications for connectional heterogeneity. *Learning & Memory*, 14(11):705–713, November 2007.

[33] Bruce L. McNaughton and Richard G. Morris. Hippocampal synaptic enhancement and information storage within a distributed memory system. *Trends in Neurosciences*, 10(10), December 1987.

[34] Michael E. Hasselmo, Bradley P. Wyble, and Gene V. Wallenstein. Encoding and retrieval of episodic memories: Role of cholinergic and GABAergic modulation in the hippocampus. *Hippocampus*, 6(6):693–708, December 1998.

[35] Sheri J. Mizumori, Bruce L. McNaughton, Carol A. Barnes, and K. B. Fox. Preserved spatial coding in hippocampal CA1 pyramidal cells during reversible suppression of CA3c output: Evidence for pattern completion in hippocampus. *The Journal of Neuroscience*, 9(11):3915–3928, November 1989.

[36] April E. Gold and Raymond P. Kesner. The role of the CA3 subregion of the dorsal hippocampus in spatial pattern completion in the rat. *Hippocampus*, 15(6):808–814, 2005.

[37] Jill K. Leutgeb, Stefan Leutgeb, May-Britt Moser, and Edvard I. Moser. Pattern Separation in the Dentate Gyrus and CA3 of the Hippocampus. *Science*, 315(5814):961–966, February 2007.

[38] Stefan Leutgeb and Jill K. Leutgeb. Pattern separation, pattern completion, and new neuronal codes within a continuous CA3 map. *Learning & Memory*, 14(11):745–757, November 2007.

[39] Marcus K. Benna and Stefano Fusi. Place cells may simply be memory cells: Memory compression leads to spatial tuning and history dependence. *Proceedings of the National Academy of Sciences*, 118(51):e2018422118, December 2021.

[40] Rajkumar Vasudeva Raju, J Swaroop Guntupalli, Guangyao Zhou, Miguel Lázaro-Gredilla, and Dileep George. Space is a latent sequence: Structured sequence learning as a unified theory of representation in the hippocampus. *arXiv preprint arXiv:2212.01508*, 2022.

[41] Daniel Levenstein, Aleksei Efremov, Roy Henha Eyono, Adrien Peyrache, and Blake Richards. Sequential predictive learning is a unifying theory for hippocampal representation and replay. *bioRxiv*, pages 2024–04, 2024.

[42] Laura Lee Colgin, Edvard I. Moser, and May-Britt Moser. Understanding memory through hippocampal remapping. *Trends in Neurosciences*, 31(9):469–477, September 2008.

[43] Edvard I. Moser, Emilio Kropff, and May-Britt Moser. Place Cells, Grid Cells, and the Brain's Spatial Representation System. *Annual Review of Neuroscience*, 31(1):69–89, July 2008.

[44] Oswald Steward and Sheila A. Scoville. Cells of origin of entorhinal cortical afferents to the hippocampus and fascia dentata of the rat. *The Journal of Comparative Neurology*, 169(3):347–370, October 1976.

[45] Daniel J. Felleman and David C. Van Essen. Distributed Hierarchical Processing in the Primate Cerebral Cortex. *Cerebral Cortex*, 1(1):1–47, January 1991.

[46] Caroline Le Duigou, Jean Simonnet, Maria T. Teleñczuk, Desdemona Fricker, and Richard Miles. Recurrent synapses and circuits in the CA3 region of the hippocampus: An associative network. *Frontiers in Cellular Neuroscience*, 7, 2014.

[47] Mikail Khona and Ila R. Fiete. Attractor and integrator networks in the brain. *Nature Reviews Neuroscience*, 23(12):744–766, December 2022.

[48] Christopher J Cueva and Xue-Xin Wei. Emergence of grid-like representations by training recurrent neural networks to perform spatial localization. *arXiv preprint arXiv:1803.07770*, 2018.

[49] Andrea Banino, Caswell Barry, Benigno Uria, Charles Blundell, Timothy Lillicrap, Piotr Mirowski, Alexander Pritzel, Martin J Chadwick, Thomas Degris, Joseph Modayil, et al. Vector-based navigation using grid-like representations in artificial agents. *Nature*, 557(7705):429–433, 2018.

[50] Ben Sorscher, Gabriel Mel, Surya Ganguli, and Samuel Ocko. A unified theory for the origin of grid cells through the lens of pattern formation. *Advances in neural information processing systems*, 32, 2019.

[51] Mark P. Brandon, Andrew R. Bogaard, Christopher P. Libby, Michael A. Connerney, Kishan Gupta, and Michael E. Hasselmo. Reduction of Theta Rhythm Dissociates Grid Cell Spatial Periodicity from Directional Tuning. *Science*, 332(6029):595–599, April 2011.

[52] Linlin Z. Fan, Doo Kyung Kim, Joshua H. Jennings, He Tian, Peter Y. Wang, Charu Ramakrishnan, Sawyer Randles, Yanjun Sun, Elina Thadhani, Yoon Seok Kim, Sean Quirin, Lisa Giocomo, Adam E. Cohen, and Karl Deisseroth. All-optical physiology resolves a synaptic basis for behavioral timescale plasticity. *Cell*, 186(3):543–559.e19, February 2023.

[53] Aviv Ratzon, Dori Derdikman, and Omri Barak. Representational drift as a result of implicit regularization, April 2024.

[54] André A. Fenton, Hsin-Yi Kao, Samuel A. Neymotin, Andrey Olypher, Yevgeniy Vayntrub, William W. Lytton, and Nandor Ludvig. Unmasking the CA1 Ensemble Place Code by Exposures to Small and Large Environments: More Place Cells and Multiple, Irregularly Arranged, and Expanded Place Fields in the Larger Space. *The Journal of Neuroscience*, 28(44):11250–11262, October 2008.

[55] EunHye Park, Dino Dvorak, and André A. Fenton. Ensemble Place Codes in Hippocampus: CA1, CA3, and Dentate Gyrus Place Cells Have Multiple Place Fields in Large Environments. *PLoS ONE*, 6(7):e22349, July 2011.

[56] Caswell Barry, Robin Hayman, Neil Burgess, and Kathryn J Jeffery. Experience-dependent rescaling of entorhinal grids. *Nature neuroscience*, 10(6):682–684, 2007.

[57] Hanne Stensola, Tor Stensola, Trygve Solstad, Kristian Frøland, May-Britt Moser, and Edvard I Moser. The entorhinal grid map is discretized. *Nature*, 492(7427):72–78, 2012.

[58] Julija Krupic, Marius Bauza, Stephen Burton, and John O'Keefe. Framing the grid: effect of boundaries on grid cells and navigation. *The Journal of physiology*, 594(22):6489–6499, 2016.

[59] Julija Krupic, Marius Bauza, Stephen Burton, and John O'Keefe. Local transformations of the hippocampal cognitive map. *Science*, 359(6380):1143–1146, 2018.

[60] Alexandra T Keinath, Ohad Rechnitz, Vijay Balasubramanian, and Russell A Epstein. Environmental deformations dynamically shift human spatial memory. *Hippocampus*, 31(1):89–101, 2021.

[61] Yoram Burak and Ila R Fiete. Accurate path integration in continuous attractor network models of grid cells. *PLoS computational biology*, 5(2):e1000291, 2009.

[62] Louis Kang and Vijay Balasubramanian. A geometric attractor mechanism for self-organization of entorhinal grid modules. *Elife*, 8:e46687, 2019.

[63] Alexandra T Keinath, Russell A Epstein, and Vijay Balasubramanian. Environmental deformations dynamically shift the grid cell spatial metric. *Elife*, 7:e38169, 2018.

[64] Eli Pollock, Niral Desai, Xue-xin Wei, and Vijay Balasubramanian. Dynamic self-organized error-correction of grid cells by border cells. *arXiv preprint arXiv:1808.01503*, 2018.

[65] Roddy M. Grieves, Selim Jedidi-Ayoub, Karyna Mishchanchuk, Anyi Liu, Sophie Renaudineau, and Kate J. Jeffery. The place-cell representation of volumetric space in rats. *Nature Communications*, 11(1):789, February 2020.

[66] Alexandra O. Constantinescu, Jill X. O'Reilly, and Timothy E. J. Behrens. Organizing conceptual knowledge in humans with a gridlike code. *Science*, 352(6292):1464–1468, June 2016.

[67] Genela Morris and Dori Derdikman. The chicken and egg problem of grid cells and place cells. *Trends in Cognitive Sciences*, 27(2):125–138, February 2023.

[68] Edmund T. Rolls. Pattern separation, completion, and categorisation in the hippocampus and neocortex. *Neurobiology of Learning and Memory*, 129:4–28, March 2016.

Supplemental Materials

1   Training details

1.1   Simulated trials and the artificial agent

An artificial agent explores simulated room(s) defined by fixed WSM signals, as defined in Section 2.2. The agent updates its behavior and samples sensory experience every 50ms. To realistically model rodent movement trajectories, we simulate a random walk, where artificial agents explore the room in a trajectory with random small drifts representing an animal's exploration interest: at every timestep, the agent randomly changes its movement speed and direction with a small probability, 0.2 and 0.3, respectively. The change in speed is randomly chosen from an $\mathcal{N}(5, 1)$ cm/s normal distribution, and the drift direction is randomly chosen from $\mathcal{N}(0, 0.05)$ rad/s.

1.2   Training Recurrent Autoencoder (RAE)

The simulated artificial agent gathers experience vectors along its trajectory. We train the RAE on 1s experience segments with a batch size of 500, sampled from a 300s 'decaying' distribution of recent events to encourage the network update in consideration of an extended history of events. For an event that is t seconds away from the current time step, the probability of it being sampled is:

$$P(t) = \frac{\left(\frac{T_s - t}{T_s}\right)^\alpha + \beta}{\sum_{j=1}^{T_s}\left(\frac{j}{T_s}\right)^\alpha + \beta} \tag{1}$$

Where T_s is the width of the sampling window, $\alpha = 3$ and $\beta = 0.5$.

Our RAE contains three layers: The first and the third layers represent the signals being projected to and read out from CA3, respectively. The hidden layer, being fully connected by recurrent connections, corresponds to CA3. The hidden-layer states, which model activation potentials of neurons, are governed by the following continuous-time equation:

$$\tau \frac{d\mathbf{v}_t}{dt} = -\mathbf{v}_t + \mathbf{W}^{rc} f(\mathbf{v}_t) + \mathbf{W}^{in} \mathbf{e}'_t + \mathbf{b} + \boldsymbol{\eta}_t \tag{2}$$

Here $f(x)$ is an activation function and τ governs the decay. $\mathbf{W}^{in}$ is the connection matrix to the hidden layer, simulating pathways entering the hippocampus. $\mathbf{W}^{rc}$ is the recurrent connectivity matrix emulating CA3 recurrent collaterals. The vector $\mathbf{b}$ is a firing bias term and $\boldsymbol{\eta}_t$ denotes Gaussian pre-activation noise. The variable $\mathbf{v}_t$ models neural activation potentials. Setting $\gamma = \frac{dt}{\tau}$ and adapting to discrete- time gives:

$$\mathbf{v}_{t+1} = \mathbf{v}_t + \Delta\mathbf{v}_t = (1 - \gamma)\mathbf{v}_t + \gamma\left[\mathbf{W}^{rc}\mathbf{h}_t + \mathbf{W}^{in}\mathbf{e}'_{t+1} + \mathbf{b} + \boldsymbol{\eta}_{t+1}\right] \tag{3}$$

$$\mathbf{h}_t = f(\mathbf{v}_t) + \boldsymbol{\xi}_t \tag{4}$$

Here we have replaced $f(\mathbf{v}_t)$ in equation (2) with equation (4), where $\mathbf{h}_t$ is the state vector of the hidden layer neurons in Hertz (Hz) and $\boldsymbol{\xi}_t$ is the post-activation noise.

The network is trained with mean-squared error without strict sparseness constraints. The loss function is:

$$\mathcal{L} = \frac{\lambda_{mse}}{D \cdot T \cdot B} \sum_{d,t,b}^{D,T,B} (\hat{e}_{d,t,b} - e_{d,t,b})^2 + \frac{\lambda_{fr}}{N} \sum_{n}^{N} \left(\sum_{t,b}^{T,B} r_{n,t,b}\right)^2 \tag{5}$$

D is the dimension of the Experience Vector (EV), T measures timesteps within a memory segment, B indicates the number of batches, and N counts nodes in the hidden layer. The term $\hat{e}_{d,t,b}$ is the d-th entry of the reconstructed EV at timestep t in batch b, while $e_{d,t,b}$ is the equivalent entry of the ground truth. The second component of the loss, $r_{n,t,b}$, denotes the firing rate of the n-th neuron at time t within batch b. Unless otherwise stated, we set $\lambda_{mse} = 0$ and $\lambda_{fr} = 200$ for our experiments.

Table 1: Network parameters

Parameter	Description	Value
n_hidden	# hidden layer nodes	1000
InputLayer	Distribution of the input layer	$\mathcal{U}(-\sqrt{k}, \sqrt{k})$, where $k = \frac{1}{\text{in\_features}}$
HiddenLayer	Distribution of the hidden layer	$\mathcal{U}(-\sqrt{k}, \sqrt{k})$, where $k = \frac{1}{\text{n\_hidden}}$
OutputLayer	Distribution of the output layer	$\mathcal{U}(-\sqrt{k}, \sqrt{k})$, where $k = \frac{1}{\text{n\_hidden}}$
dt	Time resolution	50 ms
τ	Time constant	500
$\gamma = \frac{dt}{\tau}$	Decaying factor	0.1
Optimizer	Network optimizer	Adam
learning_rate	The learning rate of RAE	0.0005
λ_{mse}	Coefficient for the mean-squared pattern completion error	1
λ_{fr}	Coefficient for the mean-squared hidden layer firing rates	200

Table 2: Training parameters

Parameter	Description	Value
N_{batch}	Number of episodic memory in each 'bout'	500
warmup_duration	The duration of experience vector before the first trial room (see Fig. 1b)	300 s
masking_ratio	The percentage we use to randomly occlude an arbitrary experience vector	$\mathcal{U}(r_{min}, r_{max})$ $r_{min} = 0$ & $r_{max} = 0.2$
α	The exponential coefficient in equation (1)	3
β	The constant term in equation (1)	0.05
spatial_resolution	How each meter in the real-world is converted into pixels in our simulated rooms	1 cm/pixel
T_w	Width of the sampling window (see Fig. 1 caption)	300 s
T_s	Length of each episodic memory	1 s
Δt	The step size of how much to move the sampling window forward	1 s

1.3 Testing RAE and visualizing hidden layer firing profiles

After training in each trial, we paused parameter updates and "recorded" the network response at every location in the room. The network continued to receive batches of partially occluded experiences with added noise, generated by a random traveling agent, as detailed in the main text. To ensure sufficient data at every location and to average out effects of random occlusions and noise, we conducted 20-minute trials repeated 20 times. Importantly, the obtained spatial maps are robust to both the duration and the number of tests since we paused parameter updates during testing.

During these tests, we recorded the firing rate (post-activation value) of each hidden layer unit at every location. We then averaged the unit's responses at each location across all previous visits. We repeated this process for all locations and hidden layer units to obtain spatial maps after.

2 Measurements and metrics

2.1 Spatial information content

We used the Spatial Information Content (SIC) [51] measured in bits to measure the strength of a cell's place-like property in terms of its spatial selectivity We discretize firing rate maps into M 30cm $\times$ 30cm bins. Each bin has a firing rate and associated probability p_m of the cell firing. The spatial

information content (SIC) is computed as:

$$SIC = \sum_{m=1}^{M} p_m \cdot \left(\frac{r_m}{\bar{r}}\right) \cdot log_2\left(\frac{r_m}{\bar{r}}\right)$$

where $\bar{r}$ is the average firing rate across bins. Bins with $r_m = 0$ are skipped in the sum (to avoid divergences in the log), but are included in the computation of the average rate $\bar{r}$.

2.2 Synapse reorganization score

We quantify synaptic adaptation as the ratio of the Frobenius norm of the change in the weight matrix to the Frobenius norm of the weight matrix prior to update:

$$\frac{||W^{old} - W^{new}||_F}{||W^{old}||_F}$$

Here, W^{old} and W^{new} represent synaptic weight matrices before and after adaptation, respectively.

3 Orthogonal spatial representations

3.1 Measurement of orthogonality

To measure how generated place-like patterns form representations of different rooms, and to what extent these representations are orthogonal, we adopted a methodology similar to that proposed by Alme et al. [21]. At the end of each trial, we converted the 100×100 cm firing rate map from a single unit into a 20×20 grid by averaging the rates within each bin to obtain a population coding vector for a room. To compute the similarity between two population vectors, X and Y, Alme et al. [21] used the mean dot product:

$$\frac{1}{N \cdot W \cdot H} \sum_{i,j,k}^{N,W,H} X_{i,j,k} Y_{i,j,k}$$

Here N is the number of units, and W and H are the bin dimensions in width and height, respectively. The dot product involves the population vector of a room as a whole. However, to provide a normalized measure of similarity for Fig. 5 in our main paper, we adopted the Pearson correlation. Pearson correlation also uses the population vector of a room as a whole, but normalizes the data to reduce the dominance of highly active units. Thus, the similarity between X and Y is calculated as:

$$\frac{\sum_{i=1}^{N \cdot W \cdot H}(X_i - \overline{X})(Y_i - \overline{Y})}{\sqrt{\sum_{i=1}^{N \cdot W \cdot H}(X_i - \overline{X})^2}\sqrt{\sum_{i=1}^{N \cdot W \cdot H}(Y_i - \overline{Y})^2}}$$

3.2 Drifting place fields and orthogonal representations

To test whether the generated representations can be used to construct cognitive maps for different enclosures, and whether these maps can be maintained over an extended period, we placed the agent in 20 rooms for 30 cycles, resulting in 600 recordings. In the main text, we compared how spatial representations in the last cycle compared to representations from previous cycles. Here, we offer a more comprehensive comparison. Suppl. Fig. 1 presents the cross-comparison of all 600 recordings, showing that recordings from the same room remain correlated even many cycles apart. Only recordings from cycle 1 show a slightly decreased correlation score, due to the incomplete formation of place fields.

As the simulated agent travels through multiple rooms over an increasing number of cycles, we observe that place cells, while reverting to their previous locations upon reentering a familiar room, may exhibit slight shifts in their locations. As the number of cycles between two trials of a single room increases, this discrepancy becomes increasingly pronounced, manifesting as a place field drift. Figure 2 depicts the drift of six randomly selected hidden layer units across 30 cycles in Room 1.
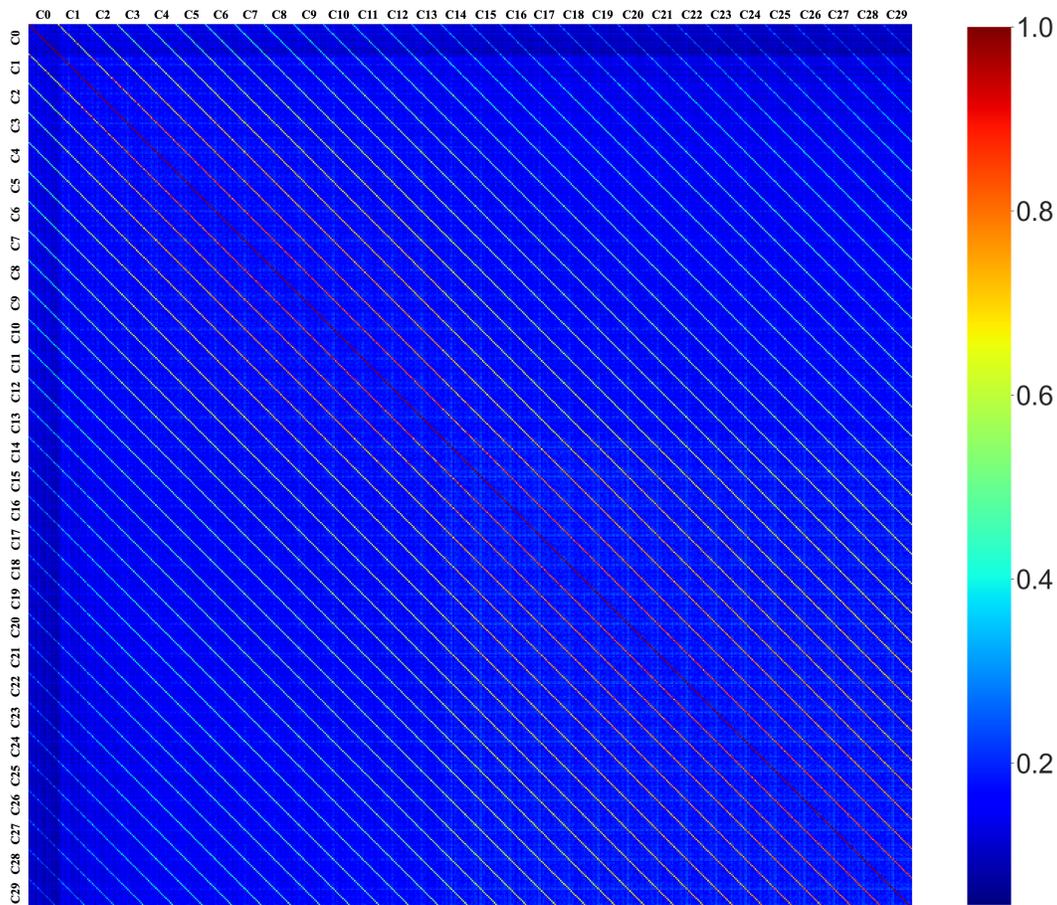
Figure 1: Cross correlation of all 600 recorded trials. Each pixel represents a comparison of two trials. During each cycle, the sequence in which the agent explores the 20 rooms is shuffled. We re-organize the room sequence when plotting the cross-correlation between trials to ease visualization. The periodic lines indicate a strong correlation of spatial representations generated when the animals entered the same room, even in different cycles.
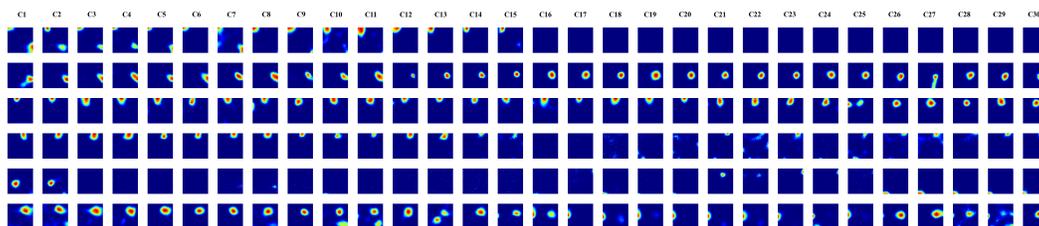

Figure 2: Illustration of place field drift across multiple visits to the same room over 30 cycles.

4 Additional results

4.1 Pattern completion results of RAE

We train the RAE to reconstruct the complete, noiseless experiences from partial and noisy sensory inputs. To examine pattern-completion performance, we pause training after each trial to record the reconstructed values and compute the average firing rate at each location for each output channel. This process is similar to the method used to gather firing profiles from the hidden layer. In Suppl. Fig. 3,

we plot 20 randomly selected WSM cells and their reconstructed values. All outputs accurately reflect the sensory changes appearing in the original WSM signals.
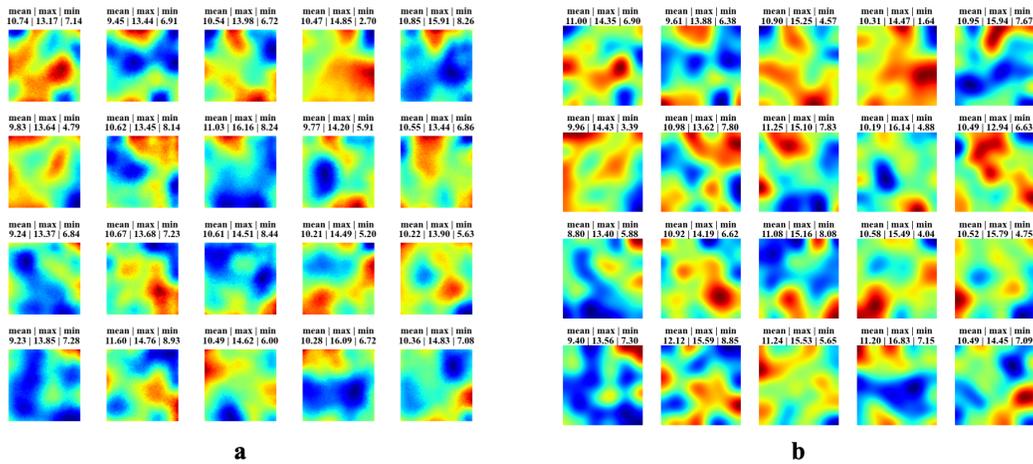

Figure 3: Example pattern completed WSM signals and their corresponding ground truths. **a.** 20 randomly selected WSM signals reconstructed by the RAE and plotted on the 2D space map. **b.** The ground truth values corresponding to the WSM cells in panel a.

4.2   Robustness to parameter variations

We have verified that the emergence of place cells is consistent across different environment shapes, for example triangles (Suppl. Fig. 4a) and circles (Suppl. Fig. 4b). In both cases, the hidden layer generated place-like patterns similar to those in the square rooms we used in our experiment.
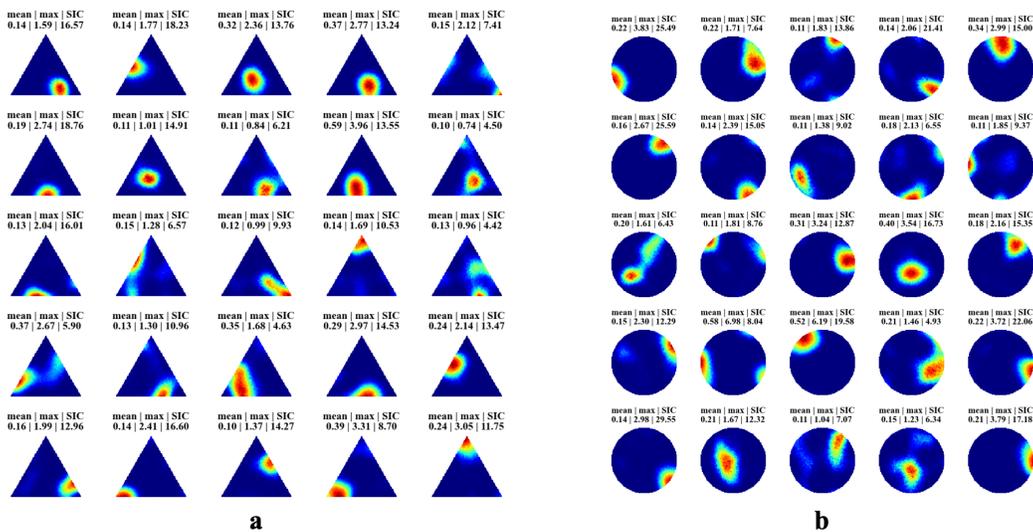

Figure 4: **a.** Example of emerged place-like patterns in a triangular room. **b.** Example of emerged place-like patterns in a circular room.

While we fixed the parameter values during our experiments to enhance reproducibility, we also verified that place cell emergence is robust to parameter changes and does not require specific values. To quantify, we evaluated the firing maps of hidden layer units using three metrics: (1) the percentage of active units, defined as units with a maximum firing rate > 0.1 Hz; (2) the percentage of place units, identified by a Spatial Information Content (SIC) > 5; (3) the average SIC across all active units.
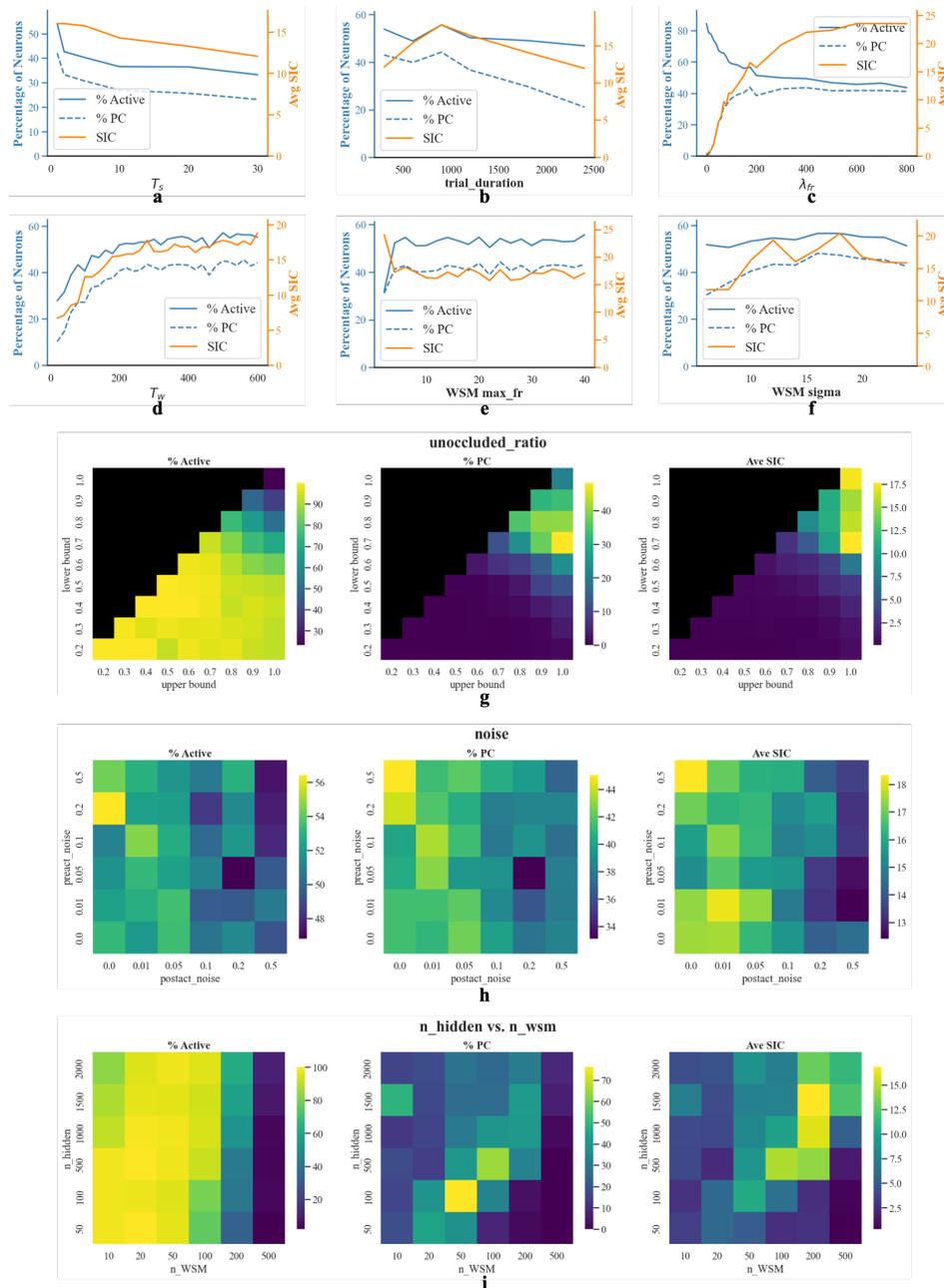
Figure 5: **a-i.** Impact of varying specific parameters, with others held constant at the default values, on place cell emergence. All experiments are conducted in a single trial room. Evaluation of hidden layer firing rate maps included three metrics: percentage of active cells (*max_fr* > 0.1 Hz) among all hidden units, percentage of place cells (*max_fr* > 0.1 Hz and SIC > 5) among all hidden units, and average SIC across active units. **a.** Duration of episodic memory segments. **b.** Total trial duration. **c.** Coefficient of firing rate loss. **d.** Warmup trial length (the recall length is also set to the same value). **e.** Maximum firing rate for each WSM channel. **f.** Sigma value for smoothing WSM signals. **g.** Ratio of unoccluded experience. We randomly preserve a fraction of the experience and train the RAE to recall the masked part, where the fraction is drawn uniformly in the interval $[r_{min}, r_{max}]$. Here we vary the bounds on this interval. **h.** Effects of pre-activation and post-activation noise. **i.** Co-varying the number of hidden units and the number of WSM cells (dimension of EV).

Figure 5 shows that: (1) Increasing the duration of each episodic memory segment slightly reduces the number of place cells, as longer episodes likely involve multiple locations, decreasing spatial specificity. Despite this, the majority of active cells continue to exhibit place-like characteristics. (see Fig. 5a). (2) The number of place cells decreases slowly as trial duration increases. This decrease is due to the optimizer forcing the network to encode WSMs more efficiently after the MSE loss stops decreasing. This optimized encoding is thus overfitted to one single room and requires individual cells to fire at unrealistic rates, which are unlikely to occur in biological systems (see Fig. 5b) (3) As λ_{fr} increases, all active cells become place cells. (4) The number of place cells and active cells increases as the recall length increases, stabilizing once the recall duration exceeds 200 seconds. (see Fig. 5d) (5) Neither the maximum firing rate of WSM signals nor the sigma value affects the emergence of PFs. (see Fig. 5e & 5f) (6) Place fields only emerge when the number of WSM signals exceeds 100, aligning with our hypothesis in the main text that the emergence of place fields requires a large number of WSM signals. We observed in our experiments that the number of hidden units required for PF emergence increases as the dimension of the experience vector (EV), i.e., the number of WSM signals, increases. This is likely because increasing the dimensionality of experience will increase the amount of information that must to be stored, and thereby require more hidden units. We leave exploration of the best ratio between input and hidden units for future work. Overall, our main finding is that the emergence of place fields is robust under a wide range of parameters.

4.3 Attractor landscape of the RAE model of place cells

Classical theories of CA3 episodic memory storage suggest that the recurrent connections establish attractor dynamics [29, 30, 28, 68]. Each attractor basin can be either a singular fixed point or a collection of points in the network's state space. Nearby network states evolve autonomously toward these attractors [47]. The attractor network theory of episodic memory also accounts for spatial memory storage, where each place-cell firing field corresponds to an attractor basin. Therefore, we also examined the attractor landscape of our RAE.
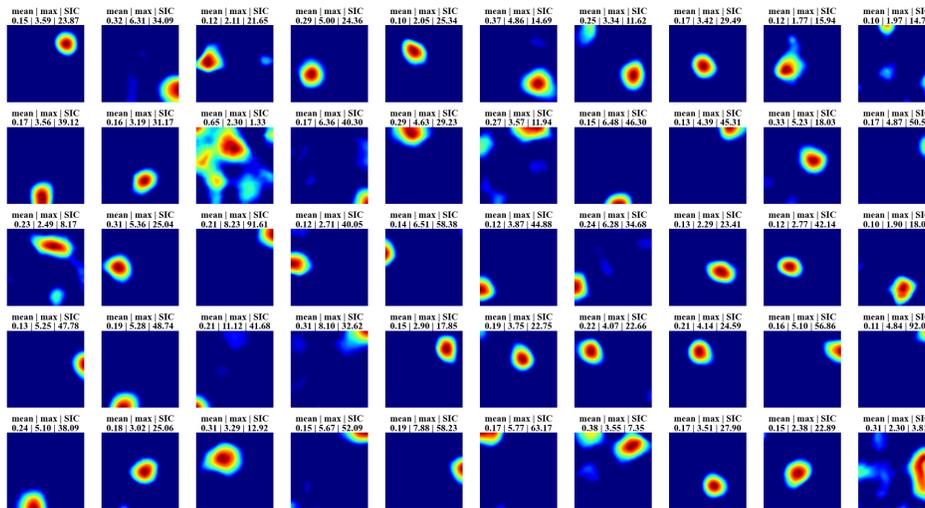

Figure 6: Example of neuronal responses at convergence points. For each location, we sample its specific EV, pause synaptic updates, and test the network by fixing this EV until convergence. Neuron states at each location are recorded upon convergence.

Attractor basins are locations where the network state becomes stable or dynamically stable. We thus examined how the network evolves when presented with a constant input. For this analysis, we simplified the network update function by removing the noise and bias terms:

$$\mathbf{v}_{t+1} = \Phi(\mathbf{v}_t) = (1 - \alpha)\mathbf{v}_t + \alpha \left[W^{rc} f(\mathbf{v}_t) + W^{in} \mathbf{e}^* \right] \tag{6}$$

where we removed the bias and noise terms to simplify the calculation. As we show below, the network state update function is a contraction, and if inputs are held constant, the network will converge to a stable state. Given this property, we can plot the attractor landscape of our RAE

network by testing the network with location-specific EVs, and waiting for convergence to the attractor at each point.

As depicted in Suppl. Fig. 6, individual units maintain place-like patterns after the network has converged. This single-unit level continuous response at convergence will also result in a continuous landscape after the network converges. Thus, our network also aligns with the classical attractor theory of place cells.

Proof. If the input to the RNN is fixed (i.e., $\forall i, j \in [0, T], i \neq j$, we have $\mathbf{e}_i = \mathbf{e}_j = \mathbf{e}^*$), where T is the length of the input sequence. We would like to prove the network update function is a contraction, i.e., the network will converge to a fixed state. We work with the network update function:

$$\mathbf{v}_{t+1} = \Phi(\mathbf{v}_t) = (1 - \alpha)\mathbf{v}_t + \alpha \left[W^{rc} f(\mathbf{v}_t) + W^{in} \mathbf{e}^* \right] . \tag{7}$$

To show that the network will converge to a fixed state, we first show that the network update function is a contraction. To do so, we need to show $\forall i, j \in [0, T], i \neq j$, if $\|\Phi(\mathbf{v}_j) - \Phi(\mathbf{v}_i)\| < k\|\mathbf{v}_j - \mathbf{v}_i\|$, where $k < 1$.

Suppose $\mathbf{v}_j - \mathbf{v}_i = \mathbf{u}$, then

$$\Phi(\mathbf{v}_j) = \Phi(\mathbf{v}_i + \mathbf{u}) = (1 - \alpha)(\mathbf{v}_i + \mathbf{u}) + \alpha \left[W^{rc} f(\mathbf{v}_i + \mathbf{u}) + W^{in} \mathbf{e}^* \right] \tag{8}$$

$$\Phi(\mathbf{v}_j) - \Phi(\mathbf{v}_i) = (1 - \alpha)\mathbf{v}_j + \alpha \left[W^{rc} f(\mathbf{v}_j) + W^{in} \mathbf{e}^* \right] - (1 - \alpha)\mathbf{v}_i - \alpha \left[W^{rc} f(\mathbf{v}_i) + W^{in} \mathbf{e}^* \right]$$
$$= (1 - \alpha)\mathbf{u} + \alpha W^{rc} \left[f(\mathbf{v}_i + \mathbf{u}) - f(\mathbf{v}_i) \right] \tag{9}$$

By the triangle inequality and submultiplicativity,

$$\|\Phi(\mathbf{v}_j) - \Phi(\mathbf{v}_i)\| \leq (1 - \alpha)\|\mathbf{u}\| + \alpha\|W^{rc}\|\|f(\mathbf{v}_i + \mathbf{u}) - f(\mathbf{v}_i)\| \tag{10}$$

Furthermore, if the activation function is bounded and is Lipschitz continuous on real numbers, a Lipschitz constant L exists such that $\|f(\mathbf{v}_i + \mathbf{u}) - f(\mathbf{v}_i)\|$ is bounded by $L\|\mathbf{u}\|$. Thus,

$$\|\Phi(\mathbf{v}_j) - \Phi(\mathbf{v}_i)\| \leq (1 - \alpha)\|\mathbf{u}\| + \alpha\|W^{rc}\|L\|\mathbf{u}\|$$
$$= (1 - \alpha + \alpha\|W^{rc}\|L)\|\mathbf{u}\| = k\|\mathbf{u}\| \tag{11}$$

The update function is a contraction mapping if $k = (1 - \alpha) + \alpha\|W^{rc}\|L < 1$. Therefore, $\|W^{rc}\| < L^{-1}$ to ensure $k < 1$. The Lipschitz constant is $L = 0.25$ for sigmoid activation, $L = 0.5$ for tanh activation, and $L = 1$ for the positive part of ReLU activation.

Because the neuronal activation potentials are real numbers and we are using the distance function as the metric, the state-space is complete. By the Banach fixed-point theorem, iteratively applying this transformation will converge to a fixed point $\mathbf{v}^*$ in the state space. $\square$

NeurIPS Paper Checklist

1. **Claims**

   Question: Do the main claims made in the abstract and introduction accurately reflect the paper's contributions and scope?

   Answer: [Yes]

   Justification: There are two claims in the abstract: 1) Training our autoencoder to pattern-complete and reconstruct sensory experiences with a constraint on total activity causes place cells to emerge in the encoding layer. 2) The emergent place fields reproduce key aspects of hippocampal phenomenology, including remapping, orthogonality of spatial representations in different rooms, robust place field emergence in differently shaped rooms, and slow representational drift of place fields. Both our conceptual framework and the results supporting the claims made in the abstract have been reported in the paper.

   Guidelines:

   - The answer NA means that the abstract and introduction do not include the claims made in the paper.
   - The abstract and/or introduction should clearly state the claims made, including the contributions made in the paper and important assumptions and limitations. A No or NA answer to this question will not be perceived well by the reviewers.
   - The claims made should match theoretical and experimental results, and reflect how much the results can be expected to generalize to other settings.
   - It is fine to include aspirational goals as motivation as long as it is clear that these goals are not attained by the paper.

2. **Limitations**

   Question: Does the paper discuss the limitations of the work performed by the authors?

   Answer: [Yes]

   Justification: We have discussed the limitation of this framework in the second to the last paragraph. The two major limitations are: 1) This paper could benefit from additional statistical comparison with rodent place cells. 2) We assumed the inherent structure of sensory signals during spatial navigation can be modeled by smooth Gaussian random fields. While this is supported by the evidence of abundant WSM cells in the medial entorhinal cortex, we invite future discussion on what composes sensory signals as well as systematic analyses on how to characterize their structures.

   Guidelines:

   - The answer NA means that the paper has no limitation while the answer No means that the paper has limitations, but those are not discussed in the paper.
   - The authors are encouraged to create a separate "Limitations" section in their paper.
   - The paper should point out any strong assumptions and how robust the results are to violations of these assumptions (e.g., independence assumptions, noiseless settings, model well-specification, asymptotic approximations only holding locally). The authors should reflect on how these assumptions might be violated in practice and what the implications would be.
   - The authors should reflect on the scope of the claims made, e.g., if the approach was only tested on a few datasets or with a few runs. In general, empirical results often depend on implicit assumptions, which should be articulated.
   - The authors should reflect on the factors that influence the performance of the approach. For example, a facial recognition algorithm may perform poorly when image resolution is low or images are taken in low lighting. Or a speech-to-text system might not be used reliably to provide closed captions for online lectures because it fails to handle technical jargon.
   - The authors should discuss the computational efficiency of the proposed algorithms and how they scale with dataset size.
   - If applicable, the authors should discuss possible limitations of their approach to address problems of privacy and fairness.

- While the authors might fear that complete honesty about limitations might be used by reviewers as grounds for rejection, a worse outcome might be that reviewers discover limitations that aren't acknowledged in the paper. The authors should use their best judgment and recognize that individual actions in favor of transparency play an important role in developing norms that preserve the integrity of the community. Reviewers will be specifically instructed to not penalize honesty concerning limitations.

3. **Theory Assumptions and Proofs**

Question: For each theoretical result, does the paper provide the full set of assumptions and a complete (and correct) proof?

Answer: [Yes]

Justification: We have made the following assumptions: 1) sensory signals during spatial navigation are weakly spatial modulated. 2) sensory signals from various cortical regions compose high-dimensional vectors of experiences, and a brief, continuous sequence of experiences constructs a 'piece' of episodic memory. 3) Hippocampus CA3 can be modeled as recurrent autoencoders that autoencodes episodic memories. While these assumptions are challenging to test directly in in-vivo brains, we provide support to these assumptions with the experimental results from an extensive body of literature.

Guidelines:

- The answer NA means that the paper does not include theoretical results.
- All the theorems, formulas, and proofs in the paper should be numbered and cross-referenced.
- All assumptions should be clearly stated or referenced in the statement of any theorems.
- The proofs can either appear in the main paper or the supplemental material, but if they appear in the supplemental material, the authors are encouraged to provide a short proof sketch to provide intuition.
- Inversely, any informal proof provided in the core of the paper should be complemented by formal proofs provided in appendix or supplemental material.
- Theorems and Lemmas that the proof relies upon should be properly referenced.

4. **Experimental Result Reproducibility**

Question: Does the paper fully disclose all the information needed to reproduce the main experimental results of the paper to the extent that it affects the main claims and/or conclusions of the paper (regardless of whether the code and data are provided or not)?

Answer: [Yes]

Justification: We have outlined the detailed structure of our network implementations and experimental settings. All parameters are reported in either the main text or the supplemental materials.

Guidelines:

- The answer NA means that the paper does not include experiments.
- If the paper includes experiments, a No answer to this question will not be perceived well by the reviewers: Making the paper reproducible is important, regardless of whether the code and data are provided or not.
- If the contribution is a dataset and/or model, the authors should describe the steps taken to make their results reproducible or verifiable.
- Depending on the contribution, reproducibility can be accomplished in various ways. For example, if the contribution is a novel architecture, describing the architecture fully might suffice, or if the contribution is a specific model and empirical evaluation, it may be necessary to either make it possible for others to replicate the model with the same dataset, or provide access to the model. In general. releasing code and data is often one good way to accomplish this, but reproducibility can also be provided via detailed instructions for how to replicate the results, access to a hosted model (e.g., in the case of a large language model), releasing of a model checkpoint, or other means that are appropriate to the research performed.

- While NeurIPS does not require releasing code, the conference does require all submissions to provide some reasonable avenue for reproducibility, which may depend on the nature of the contribution. For example
  (a) If the contribution is primarily a new algorithm, the paper should make it clear how to reproduce that algorithm.
  (b) If the contribution is primarily a new model architecture, the paper should describe the architecture clearly and fully.
  (c) If the contribution is a new model (e.g., a large language model), then there should either be a way to access this model for reproducing the results or a way to reproduce the model (e.g., with an open-source dataset or instructions for how to construct the dataset).
  (d) We recognize that reproducibility may be tricky in some cases, in which case authors are welcome to describe the particular way they provide for reproducibility. In the case of closed-source models, it may be that access to the model is limited in some way (e.g., to registered users), but it should be possible for other researchers to have some path to reproducing or verifying the results.

5. **Open access to data and code**

   Question: Does the paper provide open access to the data and code, with sufficient instructions to faithfully reproduce the main experimental results, as described in supplemental material?

   Answer: [Yes]

   The code for replication is available at: `https://zhaozewang.github.io/projects/time_makes_space`

   Guidelines:
   - The answer NA means that paper does not include experiments requiring code.
   - Please see the NeurIPS code and data submission guidelines (`https://nips.cc/public/guides/CodeSubmissionPolicy`) for more details.
   - While we encourage the release of code and data, we understand that this might not be possible, so "No" is an acceptable answer. Papers cannot be rejected simply for not including code, unless this is central to the contribution (e.g., for a new open-source benchmark).
   - The instructions should contain the exact command and environment needed to run to reproduce the results. See the NeurIPS code and data submission guidelines (`https://nips.cc/public/guides/CodeSubmissionPolicy`) for more details.
   - The authors should provide instructions on data access and preparation, including how to access the raw data, preprocessed data, intermediate data, and generated data, etc.
   - The authors should provide scripts to reproduce all experimental results for the new proposed method and baselines. If only a subset of experiments are reproducible, they should state which ones are omitted from the script and why.
   - At submission time, to preserve anonymity, the authors should release anonymized versions (if applicable).
   - Providing as much information as possible in supplemental material (appended to the paper) is recommended, but including URLs to data and code is permitted.

6. **Experimental Setting/Details**

   Question: Does the paper specify all the training and test details (e.g., data splits, hyperparameters, how they were chosen, type of optimizer, etc.) necessary to understand the results?

   Answer: [Yes]

   Justification: In the main text, we have detailed the parameters and methods used to implement the recurrent autoencoder and replicate the experiments. Furthermore, we have comprehensively included every single detail necessary for reproducing our experiments in the supplemental materials.

   Guidelines:

- The answer NA means that the paper does not include experiments.
- The experimental setting should be presented in the core of the paper to a level of detail that is necessary to appreciate the results and make sense of them.
- The full details can be provided either with the code, in appendix, or as supplemental material.

7. **Experiment Statistical Significance**

Question: Does the paper report error bars suitably and correctly defined or other appropriate information about the statistical significance of the experiments?

Answer: [Yes]

Justification: We have reported the results with standard deviations in our main text where statistical details are significant to the claims we made. For plots, all values are indicated, thus error bars have not been included.

Guidelines:

- The answer NA means that the paper does not include experiments.
- The authors should answer "Yes" if the results are accompanied by error bars, confidence intervals, or statistical significance tests, at least for the experiments that support the main claims of the paper.
- The factors of variability that the error bars are capturing should be clearly stated (for example, train/test split, initialization, random drawing of some parameter, or overall run with given experimental conditions).
- The method for calculating the error bars should be explained (closed form formula, call to a library function, bootstrap, etc.)
- The assumptions made should be given (e.g., Normally distributed errors).
- It should be clear whether the error bar is the standard deviation or the standard error of the mean.
- It is OK to report 1-sigma error bars, but one should state it. The authors should preferably report a 2-sigma error bar than state that they have a 96% CI, if the hypothesis of Normality of errors is not verified.
- For asymmetric distributions, the authors should be careful not to show in tables or figures symmetric error bars that would yield results that are out of range (e.g. negative error rates).
- If error bars are reported in tables or plots, The authors should explain in the text how they were calculated and reference the corresponding figures or tables in the text.

8. **Experiments Compute Resources**

Question: For each experiment, does the paper provide sufficient information on the computer resources (type of compute workers, memory, time of execution) needed to reproduce the experiments?

Answer: [Yes]

Justification: We have included the computer resources we used in the Supplemental materials. We didn't include this information in the main text as we have verified that our results do not depend on computational resources to replicate. Both CPU and GPU are sufficient for our proposed experiments.

Guidelines:

- The answer NA means that the paper does not include experiments.
- The paper should indicate the type of compute workers CPU or GPU, internal cluster, or cloud provider, including relevant memory and storage.
- The paper should provide the amount of compute required for each of the individual experimental runs as well as estimate the total compute.
- The paper should disclose whether the full research project required more compute than the experiments reported in the paper (e.g., preliminary or failed experiments that didn't make it into the paper).

9. **Code Of Ethics**

Question: Does the research conducted in the paper conform, in every respect, with the NeurIPS Code of Ethics https://neurips.cc/public/EthicsGuidelines?

Answer: [Yes]

Justification: Yes, our research conforms with the NeurIPS Code of Ethics in every respect.

- The answer NA means that the authors have not reviewed the NeurIPS Code of Ethics.
- If the authors answer No, they should explain the special circumstances that require a deviation from the Code of Ethics.
- The authors should make sure to preserve anonymity (e.g., if there is a special consideration due to laws or regulations in their jurisdiction).

10. **Broader Impacts**

Question: Does the paper discuss both potential positive societal impacts and negative societal impacts of the work performed?

Answer: [NA]

Justification: There is no societal impact of the work performed

Guidelines:

- The answer NA means that there is no societal impact of the work performed.
- If the authors answer NA or No, they should explain why their work has no societal impact or why the paper does not address societal impact.
- Examples of negative societal impacts include potential malicious or unintended uses (e.g., disinformation, generating fake profiles, surveillance), fairness considerations (e.g., deployment of technologies that could make decisions that unfairly impact specific groups), privacy considerations, and security considerations.
- The conference expects that many papers will be foundational research and not tied to particular applications, let alone deployments. However, if there is a direct path to any negative applications, the authors should point it out. For example, it is legitimate to point out that an improvement in the quality of generative models could be used to generate deepfakes for disinformation. On the other hand, it is not needed to point out that a generic algorithm for optimizing neural networks could enable people to train models that generate Deepfakes faster.
- The authors should consider possible harms that could arise when the technology is being used as intended and functioning correctly, harms that could arise when the technology is being used as intended but gives incorrect results, and harms following from (intentional or unintentional) misuse of the technology.
- If there are negative societal impacts, the authors could also discuss possible mitigation strategies (e.g., gated release of models, providing defenses in addition to attacks, mechanisms for monitoring misuse, mechanisms to monitor how a system learns from feedback over time, improving the efficiency and accessibility of ML).

11. **Safeguards**

Question: Does the paper describe safeguards that have been put in place for responsible release of data or models that have a high risk for misuse (e.g., pretrained language models, image generators, or scraped datasets)?

Answer: [NA]

Justification: This paper does not pose such risks.

Guidelines:

- The answer NA means that the paper poses no such risks.
- Released models that have a high risk for misuse or dual-use should be released with necessary safeguards to allow for controlled use of the model, for example by requiring that users adhere to usage guidelines or restrictions to access the model or implementing safety filters.
- Datasets that have been scraped from the Internet could pose safety risks. The authors should describe how they avoided releasing unsafe images.

- We recognize that providing effective safeguards is challenging, and many papers do not require this, but we encourage authors to take this into account and make a best faith effort.

12. **Licenses for existing assets**

    Question: Are the creators or original owners of assets (e.g., code, data, models), used in the paper, properly credited and are the license and terms of use explicitly mentioned and properly respected?

    Answer: [NA]

    Justification: All assets are created by ourselves.

    Guidelines:

    - The answer NA means that the paper does not use existing assets.
    - The authors should cite the original paper that produced the code package or dataset.
    - The authors should state which version of the asset is used and, if possible, include a URL.
    - The name of the license (e.g., CC-BY 4.0) should be included for each asset.
    - For scraped data from a particular source (e.g., website), the copyright and terms of service of that source should be provided.
    - If assets are released, the license, copyright information, and terms of use in the package should be provided. For popular datasets, `paperswithcode.com/datasets` has curated licenses for some datasets. Their licensing guide can help determine the license of a dataset.
    - For existing datasets that are re-packaged, both the original license and the license of the derived asset (if it has changed) should be provided.
    - If this information is not available online, the authors are encouraged to reach out to the asset's creators.

13. **New Assets**

    Question: Are new assets introduced in the paper well documented and is the documentation provided alongside the assets?

    Answer: [NA]

    Justification: Our paper does not release new assets.

    Guidelines:

    - The answer NA means that the paper does not release new assets.
    - Researchers should communicate the details of the dataset/code/model as part of their submissions via structured templates. This includes details about training, license, limitations, etc.
    - The paper should discuss whether and how consent was obtained from people whose asset is used.
    - At submission time, remember to anonymize your assets (if applicable). You can either create an anonymized URL or include an anonymized zip file.

14. **Crowdsourcing and Research with Human Subjects**

    Question: For crowdsourcing experiments and research with human subjects, does the paper include the full text of instructions given to participants and screenshots, if applicable, as well as details about compensation (if any)?

    Answer: or [NA]

    Justification: Our paper does not involve crowdsourcing nor research with human subjects.

    Guidelines:

    - The answer NA means that the paper does not involve crowdsourcing nor research with human subjects.
    - Including this information in the supplemental material is fine, but if the main contribution of the paper involves human subjects, then as much detail as possible should be included in the main paper.

- According to the NeurIPS Code of Ethics, workers involved in data collection, curation, or other labor should be paid at least the minimum wage in the country of the data collector.

15. **Institutional Review Board (IRB) Approvals or Equivalent for Research with Human Subjects**

Question: Does the paper describe potential risks incurred by study participants, whether such risks were disclosed to the subjects, and whether Institutional Review Board (IRB) approvals (or an equivalent approval/review based on the requirements of your country or institution) were obtained?

Answer: [NA]

Justification: Our paper does not involve crowdsourcing nor research with human subjects.

Guidelines:

- The answer NA means that the paper does not involve crowdsourcing nor research with human subjects.
- Depending on the country in which research is conducted, IRB approval (or equivalent) may be required for any human subjects research. If you obtained IRB approval, you should clearly state this in the paper.
- We recognize that the procedures for this may vary significantly between institutions and locations, and we expect authors to adhere to the NeurIPS Code of Ethics and the guidelines for their institution.
- For initial submissions, do not include any information that would break anonymity (if applicable), such as the institution conducting the review.